

Poloidal asymmetries in edge pedestals on Alcator C-Mod

C. Theiler^{1,2}, R.M. Churchill^{1,3}, I.H. Hutchinson¹, B. Lipschultz^{1,4}, P.J. Catto¹, C.S. Chang³, E. Edlund³, P. Ennever¹, D.R. Ernst¹, R. Hager³, A.E. Hubbard¹, J.W. Hughes¹, M. Landreman⁵, E.S. Marmar¹, F.I. Parra⁶, M.L. Reinke^{1,4}, J.L. Terry¹, J.R. Walk¹, D. Whyte¹,
and the Alcator C-Mod team

¹*PSFC-MIT, Cambridge, USA* ²*CRPP-EPFL, Lausanne, CH* ³*PPPL, Princeton, USA*

⁴*Department of Physics, University of York, UK* ⁵*Institute for Research in Electronics and Applied Physics, University of Maryland, USA* ⁶*Rudolf Peierls Centre for Theoretical Physics, University of Oxford, UK*

Due to the free streaming of charged particles along magnetic field lines, plasma parameters usually vary much more strongly across the field than parallel to it. In toroidally confined plasmas, quantities such as density, temperature, and plasma potential are therefore often considered to be flux functions. Different mechanisms such as fast rotation or steep radial gradients can, however, drive poloidal asymmetries. According to neoclassical theory, as the ratio of poloidal ion Larmor radius ρ_i^θ and radial scale length L_\perp increases, the quantity which usually first develops a poloidal asymmetry is the density of heavy impurities [1]. Asymmetries in other quantities are expected as well, particularly in the pedestal where ρ_i^θ/L_\perp can approach unity [1, 2]. Besides being of basic physics interest, poloidal asymmetries can have important practical consequences. The radial transport of impurities, for example, can be strongly modified by poloidal asymmetries (see e.g. [3]). In the following, we summarize recent evidence of substantial poloidal asymmetries of both the impurity and main plasma species in edge pedestals of the Alcator C-Mod tokamak.

On Alcator C-Mod, simultaneous measurements of density, velocity, and temperature of the boron minority ions are achieved across the pedestal region at both the inboard (HFS) and outboard (LFS) edge using gas puff charge exchange recombination spectroscopy (GP-CXRS) [4]. Instead of using a high-energy neutral beam as in standard CXRS, GP-CXRS uses a simple neutral gas puff to locally induce charge exchange reactions. As gas puffs can be installed almost everywhere around the periphery of the plasma, this technique opens up new possibilities to explore the poloidal structure of the edge/pedestal. On C-Mod, two systems with a complete set of toroidal and poloidal optics are operational. Their location is shown at the left of Fig. 1 together with a magnetic reconstruction of a typical C-Mod plasma. In the following, we focus on measurements obtained with these systems in I-mode and EDA H-mode plasmas, two high-confinement regimes which typically do not feature ELMs. At the right of Fig. 1, we

show some characteristic profiles for these two regimes. I-mode is a low collisionality regime ($0.1 \leq v^* \leq 1$ at the pedestal top). It features L-mode like density profiles together with a clear pedestal in temperature, and the radial temperature scale length L_T becomes comparable to ρ_i^θ , Fig. 1 (b). EDA H-mode is a high collisionality regime ($v^* \geq 1$) and features a pedestal both in density and temperature, such that L_T and L_{ne} both approach ρ_i^θ in the pedestal. These pedestals are thus well in the regime $\rho_i^\theta/L_\perp \approx 1$ where poloidal asymmetries are expected.

GP-CXRS measurements indeed reveal that isosurfaces of T_z and plasma potential Φ do not coincide in these pedestals and these quantities can therefore not simultaneously be flux functions [5]. In Fig. 2, we show radial profiles of impurity temperature T_z and radial electric field E_r at both the HFS and the LFS midplane for I-mode and EDA H-mode. In both regimes, clear temperature pedestals and E_r wells are found at the HFS and the LFS. Despite considerable freedom in the alignment of

HFS profiles relative to the LFS ones (mainly due to uncertainties in the equilibrium reconstruction), it is not possible to simultaneously align all the profiles. If we align HFS and LFS T_z profiles, the HFS E_r well is shifted out with respect to the one at the LFS by $\Delta\rho \approx 0.012$ (I-mode) and $\Delta\rho \approx 0.015$ (H-mode). If we instead align the E_r wells, the LFS temperature exceeds the temperature at the HFS by up to 70% [5].

Progress in finding a physics based alignment of HFS and LFS profiles is achieved as follows. An analysis of parallel and perpendicular heat transport time scales suggests that electron temperature is a flux function in these pedestals, while the radial heat flux estimated from global power balance is strong enough to drive poloidal asymmetries in T_i [5]. This analysis furthermore suggests that at least in H-mode, the boron population and the main ions are thermally well coupled, such that we expect that $T_i \approx T_z$. From the constancy of T_e on a flux surface and assuming a low enough friction force for the electrons, the electrons can be shown to follow the Boltzmann relation. Introducing this condition into the total (ion and electron) parallel momentum equation and neglecting contributions from the impurities results in the following relation

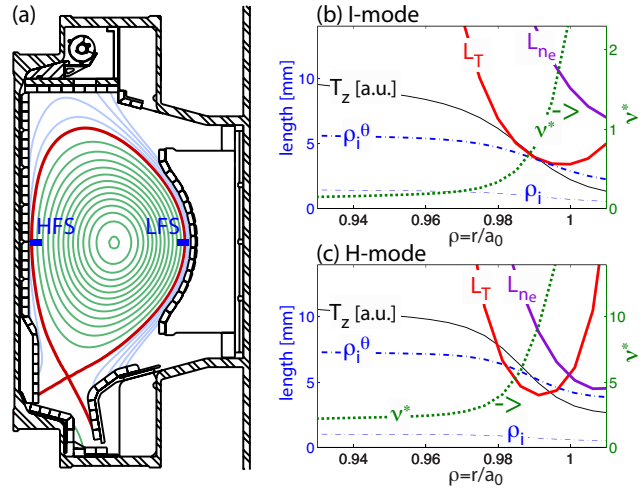


Figure 1: (a): C-Mod cross-section with GP-CXRS measurement locations indicated. (b-c): Radial edge profiles of typical I-mode and H-mode plasmas [5].

between LFS and HFS profiles [5, 6].

$$\Phi^{LFS} = \Phi^{HFS} - \frac{T_e}{e} \log \left(\frac{T_e + T_i^{LFS}}{T_e + T_i^{HFS}} \right) + \frac{T_e}{e} \log \left(\frac{p_{tot}^{LFS}}{p_{tot}^{HFS}} \right). \quad (1)$$

Here, $p_{tot} = p_e + p_i$ is the total pressure. Its poloidal variation is mainly dependent on main ion inertia and viscosity. If we assume, without complete justification, that these terms are weak, p_{tot} is a flux function and drops out of Eq. (1). In this case, Eq. (1) becomes a simple condition relating HFS and LFS profiles of T_i and Φ , or, after taking radial derivatives, profiles of T_i and E_r . We use this constraint, combined with the assumption that $T_i \approx T_z$, to align HFS and LFS profiles and

refer to it as "total pressure"-alignment in the following [6]. This alignment is applied in Fig. 2. The HFS profiles are positioned such that the HFS E_r profile estimated from the above procedure (red curve) best agrees with the actually measured HFS E_r profile. This alignment suggests that the ion temperature at the LFS substantially exceeds the HFS one in the region of steep gradients. As the HFS E_r well is slightly shifted in with respect to the one at the LFS, the plasma potential is also not constant on a flux surface. With the Boltzmann relation for electrons, this results in an electron density about twice as large in the HFS pedestal compared to the LFS [6]. Recently, a C-Mod H-mode plasma has been modeled with XGCa, a total-gyrokinetic neoclassical PIC code, an axisymmetric version of XGC1 [7]. These simulations show asymmetries qualitatively and quantitatively similar to the measurements using the "total pressure"-alignment approach [6].

In light of these substantial T_i , n_e , and Φ poloidal asymmetries on C-Mod, it does not come as a surprise that impurity density n_z also strongly varies poloidally [8]. First indications of a poloidal n_z variation in C-Mod pedestals, in this case top-out, have been obtained from passive soft x-ray emission measurements [9], with the caveat that the reported emissivity asymmetries were dependent on the accuracy of the magnetic reconstruction. More recently, an in-out n_z

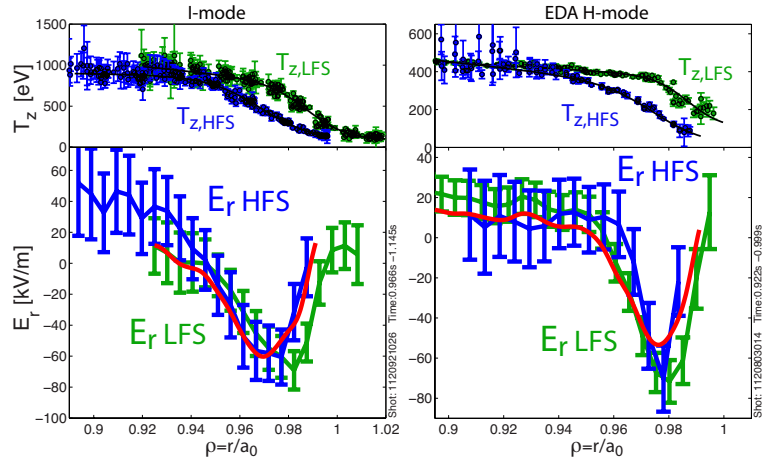


Figure 2: HFS and LFS T_z and E_r profiles in I-mode (left) and H-mode (right). The "total pressure"-alignment [6] has been used to align HFS and LFS profiles. The red curve shows the HFS E_r profile expected from this procedure.

asymmetry was inferred from the discrepancy of the measured in-out impurity flow variations compared to those expected in the case of a poloidally uniform n_z and negligible radial flows [10]. With the capability of directly measuring the HFS n_z , strong in-out asymmetries, with HFS n_z values exceeding the LFS values by up to a factor six, were demonstrated in H-mode plasmas, while asymmetries in L- and I-mode plasmas were found to be negligible [8, 6].

Comparing these findings to other machines, we note that GP-CXRS measurements on ASDEX-Upgrade reveal in-out asymmetries of impurity density in H-mode pedestals of about a factor three [11, 12], considerably weaker than on C-Mod. Furthermore, ion temperature and plasma potential were found, within error bars, to be flux functions [13]. These weaker poloidal variations than on C-Mod could be related to the lower values of ρ_i^θ/L_\perp on ASDEX-Upgrade. More recently, strong poloidal potential variations were identified in the edge of the TJ-II stellarator using Langmuir probe measurements [14].

In conclusion, in steep-gradient pedestals the impurities and the bulk plasma densities and ion temperatures can have substantial in-out asymmetries on a flux surface, with potentially important consequences for pedestal transport properties. The difference in the amplitude of these variations between C-Mod and ASDEX-Upgrade could be due to the higher values of ρ_i^θ/L_\perp in C-Mod pedestals. However, a better understanding is clearly needed to predict the importance of edge poloidal asymmetries in future devices.

This work was supported by the U.S. DOE Cooperative Agreement No. DE-FC02-99ER54512. The support from the EUROfusion Researcher Fellowship programme under grant number WP14-FRF-EPFL/Theiler is gratefully acknowledged.

References

- [1] P. Helander, Phys. Plasmas **5**, 3999 (1998)
- [2] M. Landreman and D. Ernst, Plasma Phys. Control. Fusion **54**, 115006 (2012)
- [3] C. Angioni and P. Helander, Plasma Phys. Control. Fusion **56**, 124001 (2014)
- [4] R.M. Churchill, C. Theiler, B. Lipschultz, et al., Rev. Sci. Instrum. **84**, 093505 (2013)
- [5] C. Theiler, R.M. Churchill, B. Lipschultz, et al., Nucl. Fusion **54**, 083017 (2014)
- [6] R.M. Churchill, C. Theiler, B. Lipschultz, et al., Phys. Plasmas **22**, 056104 (2015)
- [7] C.S. Chang, S. Ku, P.H. Diamond, et al., Phys. Plasmas **16**, 056108 (2009)
- [8] R.M. Churchill, B. Lipschultz, and C. Theiler, Nucl. Fusion **53**, 122002 (2013)
- [9] T.S. Pedersen, R.S. Granetz, E.S. Marmar, et al., Phys. Plasmas **9**, 4188 (2002)
- [10] K.D. Marr, B. Lipschultz, P.J. Catto, et al., Plasma Phys. Control. Fusion **52**, 055010 (2010)
- [11] T. Pütterich, E. Viezzner, R. Dux, and R.M. McDermott, Nucl. Fusion **52**, 083013 (2012)
- [12] E. Viezzner, T. Pütterich, E. Fable, et al., Plasma Phys. Control. Fusion **55**, 124037 (2013)
- [13] E. Viezzner, E. Fable, T. Pütterich, et al., Nucl. Fusion, submitted
- [14] M.A. Pedrosa, J.A. Alonso, J.M. García-Regaña, et al., Nucl. Fusion **55**, 052001 (2015)